Enhanced subterahertz spin-current transients via modulation of cross-sublattice damping in uniaxial antiferromagnets

Chi Sun [1,2,*] Hyunsoo Yang [1] and Mansoor B. A. Jalil [1]

[1] *Department of Electrical and Computer Engineering, National University of Singapore, Singapore 117576, Singapore*

[2] *Center for Quantum Spintronics, Department of Physics, Norwegian University of Science and Technology, Trondheim NO-7491, Norway*

(Received 21 December 2021; revised 15 February 2022; accepted 18 February 2022; published 7 March 2022)

We present an analytical model to compute the subterahertz (sub-THz) spin current transients injected from the insulating uniaxial antiferromagnet (AFM) into the adjacent nonmagnetic layer excited by spin pumping under the antiferromagnetic resonance condition, where both intra- and cross-sublattice damping parameters are treated on an equal footing. As expected, the sub-THz spin-pumping signal decreases with larger intra-sublattice damping dissipation. Interestingly, it is found that the amplitude of the spin current transient is enhanced with increasing cross-sublattice damping. On the other hand, the spin pumping is reduced by increasing the cross-sublattice spin-mixing conductance. These trends indicate that the intrinsic origin of the cross-sublattice damping in the bulk AFM enhances the spin current transients while its extrinsic origin, directly related to the interfacial cross-sublattice spin-mixing conductance, has the opposite effect. Our results suggest the important role of the previously neglected cross-sublattice damping in modulating the sub-THz spin current pulses for ultrafast spintronic applications.

DOI: 10.1103/PhysRevB.105.104407

I. INTRODUCTION

Antiferromagnets (AFMs) possess extremely large exchange coupling between neighboring spins, which enhances their antiferromagnetic resonance (AFMR) frequencies and enables the ultrafast spin manipulation in the potential spintronic applications [1–6]. Recently, the AFMR of uniaxial AFMs such as MnF_2 [7] and Cr_2O_3 [8] has been investigated via spin pumping, where the conversion between charge and spin at the subterahertz (sub-THz) regime has been realized. In addition to continuous harmonic excitations, the magnetization dynamics can also be manipulated by optical and magnetic pulses, from which the resulting short spin current transients can be utilized for ultrafast spintronic devices. Compared with optical lasers which induce incoherent thermal effects [9–12], spin pumping excited by magnetic pulses gives rise to coherent and pure spin current transients, which are highly desired due to lower power consumption.

In spin pumping, the magnetic material transfers angular momentum or spin current into the adjacent nonmagnetic layer (NM), where the magnetization dynamics can be modeled phenomenologically within the Landau-Lifshitz (LL) treatment with the introduction of the Gilbert damping term. For magnetic materials with two sublattices, it has been suggested that the previously disregarded cross-sublattice damping terms also play important roles, in addition to their intrasublattice counterparts [13–15]. Furthermore, it is well known that the angular momentum transferred to the conduction electrons in the NM, the extent of which is governed by the interfacial spin-mixing conductance, gives rise to enhanced Gilbert damping on top of the intrinsic damping in the bulk of the magnetic material [16,17]. Hence, the effects of the intra- and cross-sublattice damping and spin-mixing conductance terms on spin pumping should be considered simultaneously.

In this work, we present an analytical model to calculate the sub-THz spin current transients injected from the insulating uniaxial AFM (e.g., Cr_2O_3) into the adjacent NM excited by magnetic field pulses via spin pumping, where both intra- and cross-sublattice contributions are considered. As expected, the sub-THz spin-pumping signal at AFMR decreases with larger intra-sublattice damping dissipation. Interestingly, it is found that the amplitude of the spin current transient is enhanced with increasing cross-sublattice damping. On the other hand, the spin pumping is reduced by increasing the cross-sublattice mixing conductance. These trends indicate that the intrinsic cross-sublattice damping in the bulk AFM helps to enhance the spin current transients while its extrinsic counterpart, directly related to the interfacial cross-sublattice spin-mixing conductance, contributes in the opposite way. Our results suggest the important role of the cross-sublattice damping in modulating the sub-THz spin current pulses for possible ultrafast spintronic applications [18–22].

II. THEORY AND MODEL

We assume the easy axis of the uniaxial AFM is along the x axis, and a small linearly polarized magnetic field pulse $\boldsymbol{h}(t)$ is applied perpendicularly to excite the spin pumping. In the macrospin treatment with two sublattices ($i = 1, 2$), the magnetization dynamics is governed by the two coupled

*e0021580@u.nus.edu

Landau-Lifshitz-Gilbert (LLG) equations, i.e.,

$$\begin{aligned}\frac{d\boldsymbol{m}_1}{dt} &= -\mu_0\gamma[\boldsymbol{m}_1\times\boldsymbol{H}_{\text{tot},1}+\alpha_{11}\boldsymbol{m}_1\times(\boldsymbol{m}_1\times\boldsymbol{H}_{\text{tot},1})\\ &\quad+\alpha_{12}\boldsymbol{m}_1\times(\boldsymbol{m}_2\times\boldsymbol{H}_{\text{tot},2})],\\ \frac{d\boldsymbol{m}_2}{dt} &= -\mu_0\gamma[\boldsymbol{m}_2\times\boldsymbol{H}_{\text{tot},2}+\alpha_{22}\boldsymbol{m}_2\times(\boldsymbol{m}_2\times\boldsymbol{H}_{\text{tot},2})\\ &\quad+\alpha_{21}\boldsymbol{m}_2\times(\boldsymbol{m}_1\times\boldsymbol{H}_{\text{tot},1})],\end{aligned} \tag{1}$$

where $\boldsymbol{m}_i$ denotes the sublattice magnetization unit vector and μ_0 is the vacuum permeability. Since we are considering the AFM with ultralow damping, the second-order dependence of the gyromagnetic ratio γ on the damping constant is ignored for simplicity. The first term on the right-hand side of Eq. (1) represents the precession term with respect to the total magnetic field $\boldsymbol{H}_{\text{tot},i}$, which is composed of the excitation magnetic field pulse $\boldsymbol{h}(t)$ and the effective field $\boldsymbol{H}_{\text{eff},i}$ acting on sublattice i. In terms of the exchange field H_E and the uniaxial easy-axis anisotropy H_a, we have $\boldsymbol{H}_{\text{eff},1}=-H_E\boldsymbol{m}_2+H_a(\boldsymbol{m}_1\cdot\hat{\boldsymbol{x}})\hat{\boldsymbol{x}}$ and $\boldsymbol{H}_{\text{eff},2}=-H_E\boldsymbol{m}_1+H_a(\boldsymbol{m}_2\cdot\hat{\boldsymbol{x}})\hat{\boldsymbol{x}}$. Here the zero-field mode is considered, i.e., there is no external static magnetic field. The following two terms on the right-hand side of Eq. (1) pertain to the damping effect in the system. In addition to the damping constants for the intra-sublattice (i.e., α_{11} and α_{22}), we also include the cross-sublattice terms in the Gilbert damping [13], i.e., α_{12} and α_{21}. In this work, $\alpha_{12}=\alpha_{21}$ is assumed for AFM [13,23]. Since we are interested in the small-angle precession of the magnetizations, it is assumed that the lattice magnetizations are largely oriented along the uniaxial easy axis, i.e., $\boldsymbol{m}_i=(-1)^{i-1}\hat{\boldsymbol{x}}+m_{yi}\hat{\boldsymbol{y}}+m_{zi}\hat{\boldsymbol{z}}$. Here the x component is fixed since the LLG equation considers magnetization as a vector of fixed length and ignores its longitudinal relaxation. To cover the longitudinal relaxation at elevated temperatures, other theoretical approaches such as the Fokker-Planck equation [24] should be utilized in place of the LLG equation, which lies out of the scope of our current work. In this small-angle limit, the LLG equations can be linearized as

$$\frac{d}{dt}\delta\boldsymbol{m}=\mathcal{M}\delta\boldsymbol{m}+\boldsymbol{F}(t), \tag{2}$$

where the vector of the dynamic magnetization components is given by $\delta\boldsymbol{m}=(m_{y1},m_{z1},m_{y2},m_{z2})^T$. The matrices in Eq. (2) are explicitly given by

$$\mathcal{M}=\mu_0\gamma\begin{pmatrix}\alpha_{12}H_E-\alpha_{11}(H_a+H_E) & -(H_a+H_E) & \alpha_{12}(H_a+H_E)-\alpha_{11}H_E & -H_E\\ H_a+H_E & \alpha_{12}H_E-\alpha_{11}(H_a+H_E) & H_E & \alpha_{12}(H_a+H_E)-\alpha_{11}H_E\\ \alpha_{12}(H_a+H_E)-\alpha_{22}H_E & H_E & \alpha_{12}H_E-\alpha_{22}(H_a+H_E) & H_a+H_E\\ -H_E & \alpha_{12}(H_a+H_E)-\alpha_{22}H_E & -(H_a+H_E) & \alpha_{12}H_E-\alpha_{22}(H_a+H_E)\end{pmatrix} \tag{3}$$

and

$$\boldsymbol{F}(t)=\mu_0\gamma(\alpha_{11}-\alpha_{12}\quad -1\quad \alpha_{22}-\alpha_{12}\quad 1)^T\boldsymbol{h}(t). \tag{4}$$

In Eq. (4), we consider the excitation dynamic magnetic field of the form $\boldsymbol{h}(t)=h_y\exp[-\frac{(t-t_0)^2}{2\sigma^2}-i(\Omega t+\phi_h)]\hat{\boldsymbol{y}}$, i.e., the product of a Gaussian pulse with a width σ and temporal shift t_0 and a harmonic carrier with a frequency Ω and phase ϕ_h, which is linearly polarized perpendicular to the uniaxial easy axis. From Eq. (3), the AFMR frequency can be obtained as

$$\omega_r=\mu_0\gamma\sqrt{H_a(2H_E+H_a)}. \tag{5}$$

Here the two AFMR modes are degenerate in the absence of an external static magnetic field. The degeneracy can be lifted by application of an external field along the direction of the uniaxial anisotropy [25,26]. Consequently, the corresponding four complex eigenfrequencies are

$$\begin{aligned}\omega_1=\omega_3&=\sqrt{\omega_r^2-\left(\frac{\Delta\omega}{2}\right)^2}+\frac{i\Delta\omega}{2},\\ \omega_2=\omega_4&=-\sqrt{\omega_r^2-\left(\frac{\Delta\omega}{2}\right)^2}+\frac{i\Delta\omega}{2},\end{aligned} \tag{6}$$

where $\Delta\omega=\mu_0\gamma[H_E(\alpha_{11}+\alpha_{22}-2\alpha_{12})+H_a(\alpha_{11}+\alpha_{22})]$ is the resonance linewidth due to the Gilbert damping. Next, the factor $C_j=\frac{m_{y1}}{m_{y2}}$ $(j=1,\ 2,\ 3,\ 4)$ is defined to describe the eigenvector that corresponds to ω_j in Eq. (6), where we have $C_j=-\frac{\omega_j+\mu_0\gamma(H_E+H_a)}{\mu_0\gamma H_E}$. Based on the eigenvectors and eigenvalues, the fundamental matrix of the inhomogenous equation [i.e., Eq. (2)] is constructed as

$$\boldsymbol{W}(t)=\begin{pmatrix}-iC_1e^{i\omega_1t} & -iC_2e^{i\omega_2t} & iC_3e^{i\omega_3t} & iC_4e^{i\omega_4t}\\ C_1e^{i\omega_1t} & C_2e^{i\omega_2t} & C_3e^{i\omega_3t} & C_4e^{i\omega_4t}\\ -ie^{i\omega_1t} & -ie^{i\omega_2t} & ie^{i\omega_3t} & ie^{i\omega_4t}\\ e^{i\omega_1t} & e^{i\omega_2t} & e^{i\omega_3t} & e^{i\omega_4t}\end{pmatrix} \tag{7}$$

Accordingly, the final analytical solution of the transient dynamic magnetization $\delta\boldsymbol{m}$ can be calculated as

$$\begin{aligned}\delta\boldsymbol{m}&=\boldsymbol{W}(t)\int_0^t\boldsymbol{W}^{-1}(t')\boldsymbol{F}(t')dt'\\ &=\sigma\sqrt{\pi/2}\,\boldsymbol{W}(t)\boldsymbol{E}(t)\boldsymbol{S},\end{aligned} \tag{8}$$

with

$$\boldsymbol{S}=\frac{i\mu_0\gamma h_y}{2}\begin{bmatrix}\frac{\alpha_{11}-\alpha_{12}+i+C_2(\alpha_{12}-\alpha_{22}+i)}{C_1-C_2}\\ -\frac{\alpha_{11}-\alpha_{12}+i+C_1(\alpha_{12}-\alpha_{22}+i)}{C_1-C_2}\\ -\frac{\alpha_{11}-\alpha_{12}-i+C_4(\alpha_{12}-\alpha_{22}-i)}{C_3-C_4}\\ \frac{\alpha_{11}-\alpha_{12}-i+C_3(\alpha_{12}-\alpha_{22}-i)}{C_3-C_4}\end{bmatrix}. \tag{9}$$

The $\boldsymbol{E}(t)$ is a diagonal matrix with the explicit expression given by

$$\boldsymbol{E}(t)=\text{diag}(\Delta E_1,\Delta E_2,\Delta E_3,\Delta E_4), \tag{10}$$

where $\Delta E_j = E(\omega_j, t) - E(\omega_j, 0)$ with

$$E(\omega_j, t) = \exp\left[-\frac{\sigma^2}{2}(\omega_j - \Omega)^2 - it_0(\omega_j - \Omega) + i\phi_h\right] \times \text{erf}\left[\frac{t - t_0 + i\sigma^2(\omega_j - \Omega)}{\sqrt{2}\sigma}\right]. \quad (11)$$

The error function obtained above has a similar form as the dynamic magnetization transient in ferromagnetic (FM) systems [27,28].

Based on the solution of $\delta\boldsymbol{m}$ in Eq. (8), the spin-pumping current injected from the AFM into the adjacent NM can be obtained from

$$\boldsymbol{I}_{sp} = \frac{\hbar}{4\pi}\left(g_{11}\boldsymbol{m}_1 \times \frac{d\boldsymbol{m}_1}{dt} + g_{22}\boldsymbol{m}_2 \times \frac{d\boldsymbol{m}_2}{dt} + g_{12}\boldsymbol{m}_1 \times \frac{d\boldsymbol{m}_2}{dt} + g_{21}\boldsymbol{m}_2 \times \frac{d\boldsymbol{m}_1}{dt}\right), \quad (12)$$

where both the intra-sublattice spin-mixing conductance (i.e., g_{11} and g_{22}) [16,29] and the cross-sublattice terms (i.e., g_{12} and g_{21}) [15,23] are included. In the following, $g_{12} = g_{21}$ is considered [13,23]. Substituting $\boldsymbol{m}_i = (-1)^{i-1}\hat{\boldsymbol{x}} + m_{yi}\hat{\boldsymbol{y}} + m_{zi}\hat{\boldsymbol{z}}$ into Eq. (12), $\boldsymbol{I}_{sp}$ can be decomposed into two components as $\boldsymbol{I}_{sp} = \boldsymbol{I}^l_{sp} + \boldsymbol{I}^{nl}_{sp}$ with

$$\begin{aligned}\boldsymbol{I}^l_{sp} &= \frac{\hbar}{4\pi}\left[(g_{12} - g_{11})\frac{dm_{z1}}{dt} + (g_{22} - g_{12})\frac{dm_{z2}}{dt}\right]\hat{\boldsymbol{y}} \\ &\quad + \frac{\hbar}{4\pi}\left[(g_{11} - g_{12})\frac{dm_{y1}}{dt} + (g_{12} - g_{22})\frac{dm_{y2}}{dt}\right]\hat{\boldsymbol{z}} \\ &= I^{l,y}_{sp}\hat{\boldsymbol{y}} + I^{l,z}_{sp}\hat{\boldsymbol{z}} \end{aligned} \quad (13)$$

and

$$\begin{aligned}\boldsymbol{I}^{nl}_{sp} = \frac{\hbar}{4\pi}\Bigg[&g_{11}\left(m_{y1}\frac{dm_{z1}}{dt} - m_{z1}\frac{dm_{y1}}{dt}\right) \\ &+ g_{22}\left(m_{y2}\frac{dm_{z2}}{dt} - m_{z2}\frac{dm_{y2}}{dt}\right) \\ &+ g_{12}\left(m_{y1}\frac{dm_{z2}}{dt} + m_{y2}\frac{dm_{z1}}{dt} - m_{z1}\frac{dm_{y2}}{dt} - m_{z2}\frac{dm_{y1}}{dt}\right)\Bigg]\hat{\boldsymbol{x}}, \end{aligned} \quad (14)$$

where $\boldsymbol{I}^l_{sp}$ depends linearly on the time derivative of the dynamic magnetization while $\boldsymbol{I}^{nl}_{sp}$ depends on it nonlinearly. In Eq. (13), $\boldsymbol{I}^l_{sp}$ is composed of two components polarized along the two transverse directions with respect to the equilibrium magnetization or uniaxial easy axis, i.e., $I^{l,y}_{sp}$ and $I^{l,z}_{sp}$. On the other hand, $\boldsymbol{I}^{nl}_{sp}$ is completely polarized along the easy axis. In Eqs. (13) and (14), the time derivative of the dynamic magnetization can be obtained from

$$\frac{d\delta\boldsymbol{m}}{dt} = \sigma\sqrt{\pi/2}\,\boldsymbol{W}(t)\left[i\boldsymbol{\omega}\boldsymbol{E}(t) + \frac{d\boldsymbol{E}(t)}{dt}\right]\boldsymbol{S}, \quad (15)$$

with

$$\boldsymbol{\omega} = \text{diag}(\omega_1, \omega_2, \omega_3, \omega_4), \quad (16)$$

$$\frac{dE(\omega_j, t)}{dt} = \frac{1}{\sigma}\sqrt{\frac{2}{\pi}}\exp\left[-\frac{(t - t_0)^2}{2\sigma^2} - i(\omega_j - \Omega)t + i\phi_h\right]. \quad (17)$$

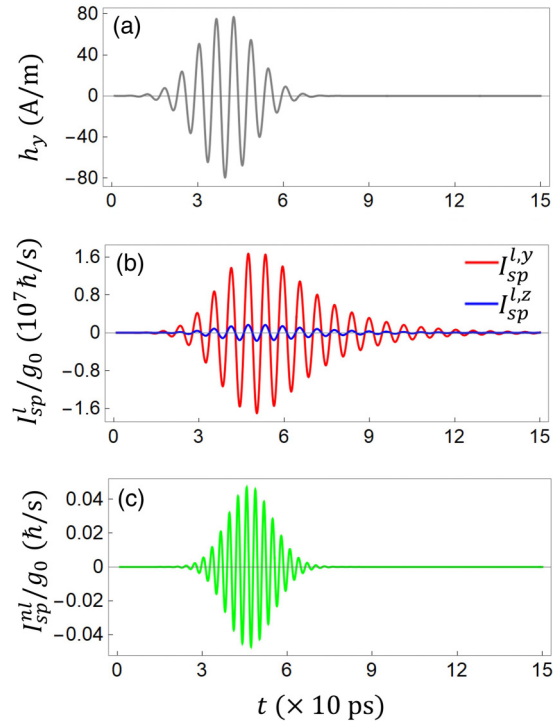

FIG. 1. Transient spin-pumping current generation when only the intra-sublattice terms are considered, i.e., $\alpha_{12} = 0$ and $g_{12} = 0$. (a) shows the excitation magnetic field pulses with two resulting spin current components $\boldsymbol{I}^l_{sp}$ in (b) and $\boldsymbol{I}^{nl}_{sp}$ in (c) at AFMR ($\Omega = \omega_r$). The red and blue lines represent the two components of $\boldsymbol{I}^l_{sp}$, i.e., $I^{l,y}_{sp}$ and $I^{l,z}_{sp}$, respectively. Note here $g_{11} = g_{22} = g_0$ is utilized and the spin-pumping current is normalized by g_0. The excitation field parameters are $\mu_0 h_y = 0.1$ mT and $\phi_h = 0$. Other parameters are $\sigma = 10$ ps and $t_0 = 40$ ps.

III. NUMERICAL RESULTS AND DISCUSSION

For numerical calculations, we assume material parameters corresponding to the uniaxial AFM Cr_2O_3 [8,30,31], i.e., $\mu_0 H_E = 245$ T, $\mu_0 H_A = 0.07$ T, and $\alpha_{11} = \alpha_{22} = 1.2 \times 10^{-3}$, yielding the AFMR frequency at $\omega_r \sim 2\pi \times 0.164$ THz, which falls within the sub-THz regime. Here a standard parameter g_0 is introduced to describe the spin-mixing conductance (e.g., g_{11}/g_0 is treated as the input parameter), whose value is canceled out for the normalized spin-pumping current $\boldsymbol{I}_{sp}/g_0$ [see Eq. (12)]. We start with the general treatment where only the intra-sublattice terms are considered, i.e., $\alpha_{12} = 0$ and $g_{12} = 0$, and the two resulting normalized spin current components $\boldsymbol{I}^l_{sp}$ and $\boldsymbol{I}^{nl}_{sp}$ excited at AFMR ($\Omega = \omega_r$) are plotted in Fig. 1. The resulting spin-pumping current is excited after the onset of the magnetic field pulse with the oscillations damping out over the timescale of the intra-sublattice damping. As shown in Fig. 1(b), the two linear spin current components share the same oscillation frequency while $I^{l,y}_{sp}$ (blue line) possesses a much larger amplitude compared with $I^{l,z}_{sp}$ (red line). On the other hand, the nonlinear spin current $\boldsymbol{I}^{nl}_{sp}$ has a negligible amplitude (i.e., more than eight orders of magnitude smaller than the linear

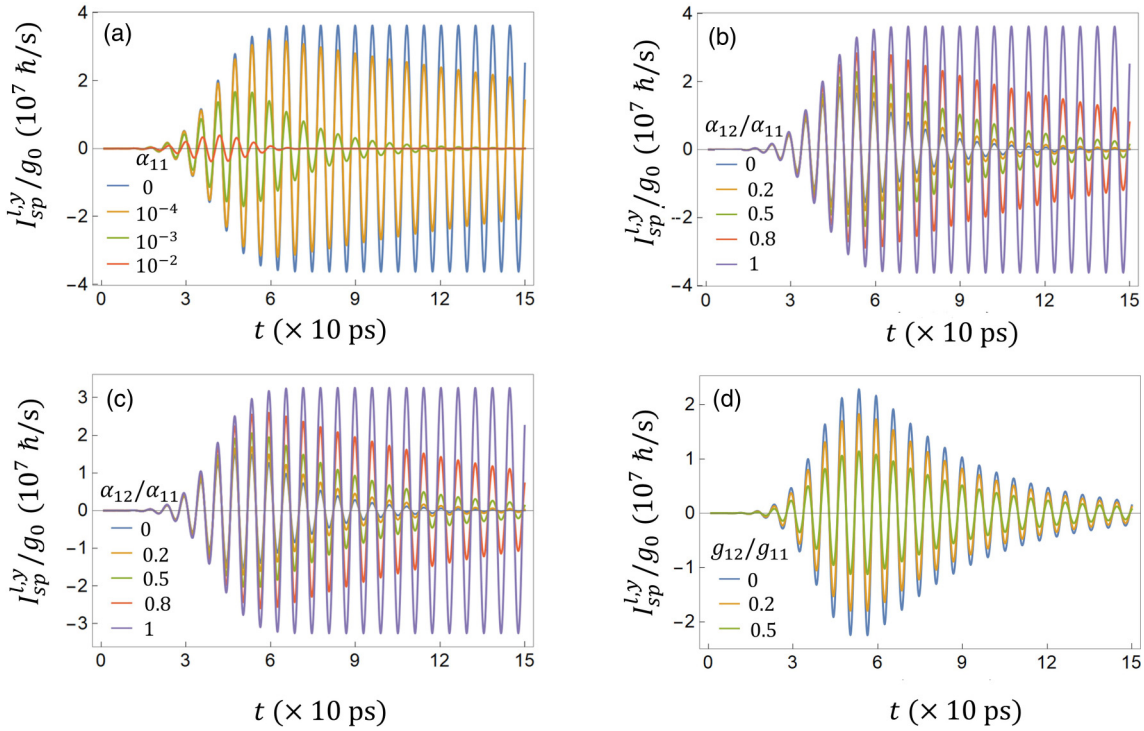

FIG. 2. The dominant linear spin-pumping current transient $I_{sp}^{l,x}$ generated at AMFR (i.e., $\Omega = \omega_r$) with different cross-sublattice parameters. (a) depicts the intra-sublattice damping dependence of $I_{sp}^{l,x}$ with $\alpha_{12} = 0$ and $g_{12} = 0$. The intrinsic cross-sublattice damping dependence of $I_{sp}^{l,x}$ is plotted in (b) with $g_{12} = 0$ and the inclusion of extrinsic cross-sublattice damping due to spin pumping is shown in (c) with $g_{12} = 0.1g_{11}$. (d) shows $I_{sp}^{l,x}$ with different cross-sublattice spin-mixing conductance values when $\alpha_{12} = 0.5\alpha_{11}$. Other parameters are the same as in Fig. 1.

counterpart) but even higher oscillation frequency compared to the excitation field. This amplitude suppression can be qualitatively explained from the additional dynamical magnetization component multiplied to the time derivative of the magnetization [see Eq. (14)], whose magnitude is much smaller than 1. Therefore, we will focus on the dominant $I_{sp}^{l,y}$ component in the following discussions.

Next, we investigate the magnetic damping dependence of the spin current transients. In Fig. 2(a), $I_{sp}^{l,y}$ is plotted with different intra-sublattice damping values (i.e., α_{11}), where the cross-sublattice damping α_{12} is excluded (i.e., $\alpha_{12} = 0$). As expected, a low damping constant is desired for spin pumping, i.e., the signal amplitude decreases with larger intra-sublattice damping dissipation in Fig. 2(a). This shares the same trend as that of spin pumping in FM systems measured by the inverse spin Hall effect [32,33]. On the other hand, in addition to the intrinsic bulk contribution, another (extrinsic) source of the magnetic damping comes from spin pumping, which is proportional to the corresponding interfacial spin-mixing conductance [16,17]. Here we treat the total Gilbert damping as a variable which includes both intrinsic and extrinsic origins. Therefore, $\alpha_{12} = 0$ is assumed in Fig. 2(a), which indicates $g_{12} = 0$ or zero extrinsic spin-pumping contribution.

Now we focus on the cross-sublattice damping, which has been largely disregarded in magnetization dynamical studies although it is suggested to play important roles [13,23]. The damping matrix including both intra- and cross-sublattice damping terms is captured by the Rayleigh dissipation functional, in which the positivity of the dissipation entails $\alpha_{11}\alpha_{22} \geqslant \alpha_{12}\alpha_{21}$ [13]. Therefore, $0 \leqslant \alpha_{12}/\alpha_{11} \leqslant 1$ should be fulfilled when investigating the α_{12} dependence. As mentioned before, $\alpha_{11} = \alpha_{22} = 1.2 \times 10^{-3}$ is assumed for the uniaxial AFM Cr_2O_3 system [8,30,31]. In order to analyze the effect of the intrinsic cross-sublattice damping separately, $I_{sp}^{l,y}$ is plotted for different α_{12} values with $g_{12} = 0$ in Fig. 2(b). Interestingly, it is found that the signal amplitude increases with the intrinsic α_{12}, which constitutes an opposite trend compared to that of its intra-sublattice counterpart. However, this trend is in line with the linewidth expression $\Delta\omega = \mu_0\gamma[H_E(\alpha_{11} + \alpha_{22} - 2\alpha_{12}) + H_a(\alpha_{11} + \alpha_{22})]$, in which $\alpha_{11}(\alpha_{22})$ and α_{12} possess contributions with opposite signs. Subsequently, the extrinsic cross-sublattice damping due to spin pumping is included in Fig. 2(c) by introducing a nonzero interfacial spin-mixing conductance, e.g., $g_{12} = 0.1g_{11}$. When α_{12} has the spin pumping induced component in addition to the intrinsic bulk value, the increasing trend of the spin current amplitude with respect to α_{12} is maintained but with a reduced amplitude compared with the case in Fig. 2(b) where α_{12} has a purely intrinsic origin. Additionally, we fix $\alpha_{12} = 0.5\alpha_{11}$ and investigate the g_{12} dependence by plotting $I_{sp}^{l,y}$ with different g_{12} values in Fig. 2(d). It is shown that $I_{sp}^{l,y}$ is reduced by increasing g_{12}, indicating the sublattice magnetizations restrict the spin current pumped by each other. This effect has been explained quantum mechanically by Kamra and Belzig [15], which further elucidates the role of the extrinsic component of α_{12} in curtailing the spin-pumping transients in Fig. 2(c). As a result, in order to enhance the transient spin current, AFM material with a large intrinsic

bulk α_{12} and the AFM/NM interface with a negligible g_{12} are desired. In practice, it has been proposed that the interface with vanishing cross-sublattice spin-mixing conductance can be achieved when only one sublattice type is exposed to the NM [23]. However, further studies are required regarding the fine modulation of both the intrinsic and extrinsic components of α_{12} .

IV. CONCLUSION

In summary, we have presented an analytical model to compute the transient spin-pumping current excited by a sub-THz magnetic field pulse from insulating uniaxial AFMs under AFMR, which treats on an equal footing both the intra- and cross-sublattice damping parameters, the latter being largely disregarded in previous studies. As expected, a low damping constant is desired for spin pumping with lower dissipation; i.e., the spin current transient decreases with increasing intra-sublattice damping. Interestingly, the oft-neglected cross-sublattice damping can contribute in the opposite way; i.e., a larger intrinsic cross-sublattice damping actually gives rise to an enhanced signal amplitude. The role of this cross-sublattice damping is rather complex, with its extrinsic component arising from the cross-sublattice spin-mixing conductance at the AFM interfaces suppressing the spin current transient. Therefore, an AFM system with a larger intrinsic cross-sublattice damping and negligible cross-sublattice spin-mixing conductance at its interfaces is desired for enhancing the output sub-THz signal. Our results suggest the important role of the cross-sublattice damping in modulating the sub-THz spin current transients for possible ultrafast spintronic applications.

ACKNOWLEDGMENTS

This work is supported by the Ministry of Education (MOE) Tier-II Grant No. MOE2018-T2-2-117 (NUS Grants No. R-263-000-E45-112 and No. R-398-000-092-112) and MOE Tier-I FRC grant (NUS Grant No. R-263-000-D66-114). H.Y. is supported by the Agency for Science, Technology and Research (A*STAR) under its AME Individual Research Grants (Grant No. A1983c0037) and National Research Foundation (NRF) Singapore Investigatorship (Grant No. NRFI06-2020-0015).

[1] V. Baltz, A. Manchon, M. Tsoi, T. Moriyama, T. Ono, and Y. Tserkovnyak, Rev. Mod. Phys. **90**, 015005 (2018).
[2] R. Cheng, D. Xiao, and A. Brataas, Phys. Rev. Lett. **116**, 207603 (2016).
[3] H. Qiu, L. Zhou, C. Zhang, J. Wu, Y. Tian, S. Cheng, S. Mi, H. Zhao, Q. Zhang, D. Wu *et al.*, Nat. Phys. **17**, 388 (2021).
[4] X. Martí, I. Fina, and T. Jungwirth, IEEE Trans. Magn. **51**, 1 (2015).
[5] K. Olejník, T. Seifert, Z. Kašpar, V. Novák, P. Wadley, R. P. Campion, M. Baumgartner, P. Gambardella, P. Němec, J. Wunderlich *et al.*, Sci. Adv. **4**, eaar3566 (2018).
[6] S. M. Rezende, A. Azevedo, and R. L. Rodríguez-Suárez, J. Appl. Phys. **126**, 151101 (2019).
[7] P. Vaidya, S. A. Morley, J. van Tol, Y. Liu, R. Cheng, A. Brataas, D. Lederman, and E. Del Barco, Science **368**, 160 (2020).
[8] J. Li, C. B. Wilson, R. Cheng, M. Lohmann, M. Kavand, W. Yuan, M. Aldosary, N. Agladze, P. Wei, M. S. Sherwin *et al.*, Nature (London) **578**, 70 (2020).
[9] Y. Wu, M. Elyasi, X. Qiu, M. Chen, Y. Liu, L. Ke, and H. Yang, Adv. Mater. **29**, 1603031 (2017).
[10] M. Chen, R. Mishra, Y. Wu, K. Lee, and H. Yang, Adv. Opt. Mater. **6**, 1800430 (2018).
[11] T. Seifert, S. Jaiswal, U. Martens, J. Hannegan, L. Braun, P. Maldonado, F. Freimuth, A. Kronenberg, J. Henrizi, I. Radu *et al.*, Nat. Photonics **10**, 483 (2016).
[12] C. Sun, S. M. Rafi-Ul-Islam, H. Yang, and M. B. A. Jalil, Phys. Rev. B **102**, 214419 (2020).
[13] A. Kamra, R. E. Troncoso, W. Belzig, and A. Brataas, Phys. Rev. B **98**, 184402 (2018).
[14] C. Sun, H. Yang, and M. B. A. Jalil, Phys. Rev. B **102**, 134420 (2020).
[15] A. Kamra and W. Belzig, Phys. Rev. Lett. **119**, 197201 (2017).
[16] Y. Tserkovnyak, A. Brataas, and G. E. W. Bauer, Phys. Rev. B **66**, 224403 (2002).
[17] Y. Tserkovnyak, A. Brataas, and G. E. W. Bauer, Phys. Rev. Lett. **88**, 117601 (2002).
[18] J. Walowski and M. Münzenberg, J. Appl. Phys. **120**, 140901 (2016).
[19] K. Cai, Z. Zhu, J. M. Lee, R. Mishra, L. Ren, S. D. Pollard, P. He, G. Liang, K. L. Teo, and H. Yang, Nat. Electron. **3**, 37 (2020).
[20] A. Schellekens, K. Kuiper, R. De Wit, and B. Koopmans, Nat. Commun. **5**, 1 (2014).
[21] Y. Yang, R. B. Wilson, J. Gorchon, C.-H. Lambert, S. Salahuddin, and J. Bokor, Sci. Adv. **3**, e1603117 (2017).
[22] C. Sun, J. Deng, S. M. Rafi-Ul-Islam, G. Liang, H. Yang, and M. B. A. Jalil, Phys. Rev. Appl. **12**, 034022 (2019).
[23] R. E. Troncoso, M. A. Lund, A. Brataas, and A. Kamra, Phys. Rev. B **103**, 144422 (2021).
[24] D. A. Garanin, Phys. Rev. B **55**, 3050 (1997).
[25] F. Keffer and C. Kittel, Phys. Rev. **85**, 329 (1952).
[26] C. Kittel, Phys. Rev. **82**, 565 (1951).
[27] L. Bocklage, J. Magn. Magn. Mater. **429**, 324 (2017).
[28] L. Bocklage, Sci. Rep. **6**, 1 (2016).
[29] A. Brataas, G. E. Bauer, and P. J. Kelly, Phys. Rep. **427**, 157 (2006).
[30] S. Foner, Phys. Rev. **130**, 183 (1963).
[31] H. Wang, C. Du, P. C. Hammel, and F. Yang, Phys. Rev. B **91**, 220410(R) (2015).
[32] K. Ando, S. Takahashi, J. Ieda, Y. Kajiwara, H. Nakayama, T. Yoshino, K. Harii, Y. Fujikawa, M. Matsuo, S. Maekawa *et al.*, J. Appl. Phys. **109**, 103913 (2011).
[33] H. Nakayama, K. Ando, K. Harii, T. Yoshino, R. Takahashi, Y. Kajiwara, K.-I. Uchida, Y. Fujikawa, and E. Saitoh, Phys. Rev. B **85**, 144408 (2012).